ISSN 1028-334X, Doklady Earth Sciences, 2007, Vol. 413, No. 2, pp. 238–243. © Pleiades Publishing, Ltd., 2007.
Original Russian Text © L.V. Solov'eva, 2007, published in Doklady Akademii Nauk, 2007, Vol. 412, No. 6, pp. 804–809.

GEOCHEMISTRY

Reworking of the Lithospheric Mantle of the Siberian Craton by Reduced Fluids in the Middle Paleozoic Kimberlite Event: Geochemical Consequences

L. V. Solov'eva

Presented by Academician F.A. Letnikov, March 30, 2006

Received April 13, 2006

DOI: 10.1134/S1028334X07020237

Nowadays, it is commonly accepted that kimberlitic magmatism of ancient platforms was initiated by hot plumes that ascended toward the base of the continental lithosphere from the Earth's deep-seated boundary sources such as the lower mantle/core boundary or transitional zone [1, 2]. The Late Devonian kimberlitic magmatism, the most productive for diamonds at the Siberian Craton, is related to the Yakutian superplume [2]. It is suggested that the plume approaching the base of a rigid continental plate produces asthenospheric melts and related assemblages of low-Cr megacrystals. The melts replace substance of the upper asthenospheric layer and the lower lithosphere. This process is rather well studied based on geochemistry of megacrystals and high-temperature deformed peridotites from kimberlites in South Africa and Yakutia [1, 3, 4].

The geochemical implications of these processes for the lithospheric mantle, which overlies the zone directly affected by the asthenospheric melt, have remained poorly studied. As was shown in [5, 6], the zonal distribution of major and minor elements at margins of garnet crystals in granular lherzolites and harzburgites from kimberlites of South Africa is a result of interaction with fluids just before their entrapment by kimberlites. Thus, the zonality is probably related to the influence of plumes rising to the base of the lithosphere.

We checked the previously proposed hypothesis on the reworking of mantle substance by reduced fluids derived from asthenospheric melts at the early stage of the kimberlite-forming cycle [7]. This hypothesis has been supported by Fe^{3+} contents in polychrome olivines found in some xenoliths of granular peridotite in the Udachnaya kimberlite pipe [8]. The cores of olivine grains, grain blocks, and particular olivine grains in such xenoliths have orange, brownish pink, brown, and yellow colors grading into green, pale green, and colorless zones. In some cases, isolated orange and yellow grains are incorporated into the groundmass of green, pale green, and colorless olivine. As has been established with Moessbauer spectroscopy, the orange, brownish, and yellow olivines contain an appreciable Fe^{3+} admixture, which is virtually missing in pale green and colorless varieties [8]. This phenomenon has been explained by nonuniform reworking of the lithospheric mantle by reduced fluids shortly before the entrapment of xenoliths by the kimberlitic melt. The xenoliths with orange, brownish, and yellow olivines are extremely rare in the population of peridotitic xenoliths in the Udachnaya pipe. The xenoliths with polychrome olivine are more frequent. The green, pale green, and colorless olivines are predominant. The color of garnet grains corresponds to that of olivines. The xenoliths with orange or polychrome olivines contain reddish violet and pink-violet garnets, while indigo blue, lilac, and inky garnets are associated with green and colorless olivines.

We chose three control groups of granular garnet peridotites (lherzolites and harzburgites) from the Udachnaya pipe: (1) xenoliths with orange, brownish pink, and yellow olivine grains (50–90% of the olivine groundmass); (2) xenoliths with polychrome olivines, in which orange and brownish pink cores and grains compose 10–25% of the olivine groundmass, and the remainder comprises green and colorless varieties; and (3) xenoliths with green, pale green, and colorless olivine grains, among which the yellowish gray variety accounts for 3–10%. The control group included three xenoliths, for which the Fe^{3+} content in olivine was measured with Moessbauer spectroscopy [8]. Data on the geochemistry of rocks and minerals from five xenoliths were reported in [9]. The chosen xenoliths have been examined carefully under a binocular microscope

---

Institute of the Earth's Crust, Siberian Division, Russian Academy of Sciences, ul. Lermontova 128, Irkutsk, 664033 Russia; e-mail: solv777@crust.irk.ru

and in thin sections. The major oxides in minerals were determined with a JEOL Superprobe 733 microprobe at the Institute of Geochemistry, Siberian Division, Russian Academy of Sciences. Concentrations of trace elements (Rb, Sr, Ba, Nb, Zr, Hf, Ti, La, Ce, Nd, Sm, Eu, Gd, Dy, Er, Yb, and Y) in garnet and clinopyroxene were measured with secondary-ion mass spectrometry at the Institute of Microelectronics, Yaroslavl. This method provided accuracy of measurements not worse than 10% for trace elements with a concentration of >1 ppm and not worse than 15–20% for concentrations ranging from 1.0 to 0.1 ppm.

The garnet lherzolite and harzburgite xenoliths from the Udachnaya pipe are common granular peridotites that do not reveal any indications of cataclasis typical of deformed peridotites from kimberlites. For each sample, the modal compositions of the main mineral assemblage (i.e., the contents of orange, brownish, and yellow olivine grains in the total amount of olivine in rock) and the character of secondary alterations of the rock are given below (in %).

Sample 343/87, garnet lherzolite: a single plate of Phl I, 10.7 Gr, 0.3 Cpx, 20 Opx, and 69 Ol (90% of olivines are pinkish, brown, and yellowish gray varieties). $Fe^{3+}/Fe_{tot} = 0.025$ in pinkish brown olivine [8]. The xenolith is slightly serpentinized (5–7%).

Sample 545/80*, garnet harzburgite: 3–7 Gr, 5–10 Opx, and 85 Ol (approximately 50% of olivines are orange and grayish yellow varieties). $Fe^{3+}/Fe_{tot} = 0.034$ in orange olivine [8]. The xenolith is intensely serpentinized (50–60%).

Sample 45/82, garnet lherzolite: 1.6 Gr, 8 Cpx, 24.2 Opx, 66.2 Ol (approximately 50% of olivines are orange and greenish yellow varieties). The xenolith contains no more than 1–3% superimposed minerals of the late metasomatic assemblage (kelyphitic phase, phlogopite II, amphibole, calcite, and ore mineral).

Sample 50/82*, garnet lherzolite: 13 Gr, 10 Cpx, 22 Opx, and 55 Ol (10% orange and 40% pinkish brown varieties). The rock contains no more than 1–3% of superimposed minerals.

Sample 325/87, garnet lherzolite: 18 Gr, 2 Cpx, 29 Opx, and 51 Ol (25% orange and pinkish brown varieties). $Fe^{3+}/Fe_{tot} = 0.020$ and 0.008 in orange and green olivines, respectively [8]. The rock is moderately serpentinized (25%).

Sample 544/80*, garnet lherzolite: 8 Gr, <1 Cpx, 15 Opx, and 75 Ol (colorless variety). The rock is intensely serpentinized (50–60%).

Sample 42/82, garnet lherzolite: 6.5 Gr, 2.5 Cpx, 23 Opx, and 68 Ol (10% pale orange grains, the remainder is pale green and colorless grains). The rock contains no more than 1–3% of superimposed minerals.

Sample 43/82, garnet lherzolite: 3.4 Gr, 3 Cpx, 18.9 Opx, and 74.7 Ol (pale green and colorless varieties). The rock contains no more than 1–3% of superimposed minerals.

Sample 00/212, garnet lherzolite: 6.8 Gr, 0.3 Cpx, 25 Opx, and 67.9 Ol (5–10% yellowish grains, the remainder is pale green and colorless olivine). The rock is slightly serpentinized (10–15%).

Sample 03/108*, garnet harzburgite: 12 Gr, 18 Opx, and 70 Ol (green, pale green, and colorless).

In the samples designated with an asterisk, the modal composition was estimated tentatively along the lines in lump specimens; in other samples, the modal composition was calculated based on proportions of grains in crushed samples. Sporadic, strongly deformed orthopyroxene megacrystals 7–20 mm in size occur in samples 343/87 and 00/212. A very small amount (<0.5%) of irregular interstitial segregations of Al–Cr spinel, often as myrmekitic intergrowth with clinopyroxene, occur in most garnet lherzolite samples. The relationships between minerals indicate that the Al–Cr spinel postdated the main mineral assemblage and predated the metasomatic assemblage [7].

The table presents the major and rare element contents in garnet and clinopyroxene from the rocks of groups 1–3. Figure 1 shows the distribution of chondrite-normalized Nb, Zr, Hf, Ti, (Y + REE), and REE contents. The chemical composition of garnet in all three groups does not reveal marked differences. The elevated FeO content in sample 45/82 (group 1) and overall enrichment of garnets pertaining to group 3 in CaO are noted. In contrast to garnet, clinopyroxene demonstrates a progressive depletion in Al_2O_3, Cr_2O_3, FeO, and Na_2O from group 1 to group 3 concurrently with appearance of the Al–Cr spinel.

The contents of all incompatible rare elements, except Rb in garnet and Rb and Ba in clinopyroxene, decrease from the rocks with orange and yellow olivines to the rocks with pale green and colorless olivines. The exceptions for Rb and Ba are probably caused by the fact that these elements were omitted in some samples. The depletion in rare elements is extremely nonuniform. The LREE (especially Nd and Sm) contents in garnet change by two to three orders of magnitude, whereas the Nb and Yb contents in garnet from all groups remain virtually unchanged. Clinopyroxene becomes depleted in all rare elements; the greatest difference (by more than 4 orders) is established for Nd and Sm. The shape of curves in lines changes drastically: instead of Nb, (Zr + Hf), and Ti minimums in clinopyroxene of group 1, low peaks of these elements appear in this mineral of group 3. The (Zr + Hf) and Ti minimums typical of the garnet pertaining to group 1 with orange and yellow olivines are commonly absent in the garnet belonging to group 3 with green and colorless olivines, and low peaks of these elements appear instead of minimums. The lines of minerals from xenoliths of the transitional group 2 occupy an intermediate position between the lines of minerals pertaining to groups 1 and 3. The distribution of rare elements in garnet from sample 50/82 and clinopyroxene from samples 50/82 and 325/87 is similar to that of minerals from

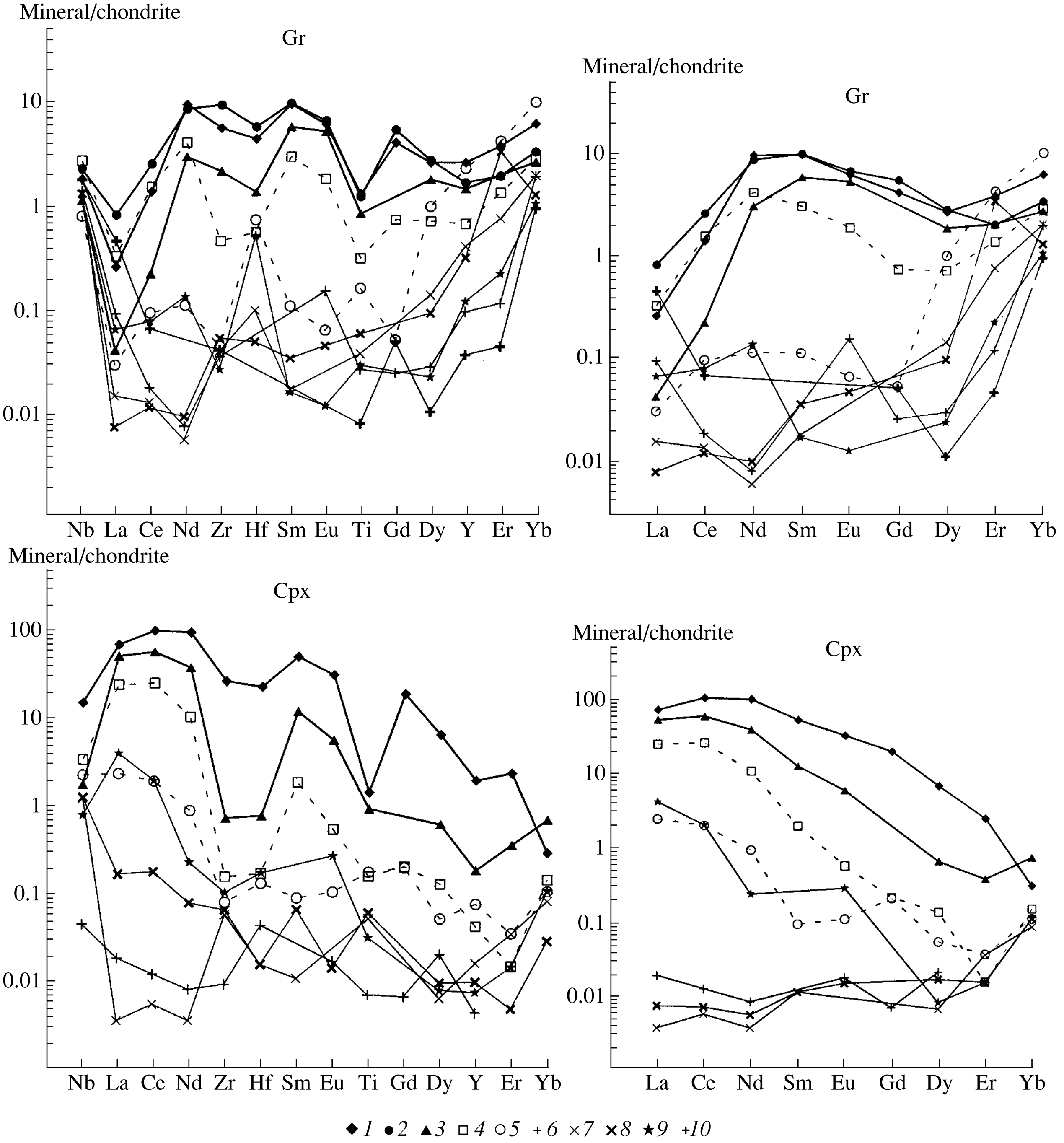

Fig. 1. Chondrite-normalized [10] HFSE (Nb, Zr, Hf, Ti), (Y + REE), and REE contents in garnet and clinopyroxene from granular garnet peridotites with olivines of different colors. Samples: (*1*) 343/87, (*2*) 545/80, (*3*) 45/82, (*4*) 50/82, (*5*) 325/87, (*6*) 544/80, (*7*) 42/82, (*8*) 43/82, (*9*) 00/212, (*10*) 03/108. Samples of group 1 are shown by a thick line; group 2, by a dashed line; and group 3, with a thin line.

group 1, whereas the garnet from sample 325/87 is closer in this respect to garnets of group 3 both in the level of contents and in their distribution. Garnets of group 1 and garnets from sample 50/82 (group 2) reveal sinusoidal REE patterns characteristic of garnet from granular peridotites [5, 6, 11].

Figure 2 shows the coefficients of rare element partition between garnet and clinopyroxene in the studied samples, as well as (DGr/Cpx) values calculated from the literature data. The DGr/Cpx curves for the samples of groups 1 and 2 are generally parallel to the theoretical curves. However, lines of group 1 lie below the theoretical curves and lines of group 2 (Fig. 2a). The lines are broken for the rocks of group 3 and are appreciably less consistent with the calculated curves (Fig. 2b).

Major (wt %) and trace elements (ppm) in garnet and clinopyroxene from granular peridotites containing olivine of different colors

Component	Garnet										Clinopyroxene							
	Group 1			Group 2		Group 3					Group 1		Group 2		Group 3			
	343/87	545/80	45/82	50/82	325/87	544/80	42/82	43/82	00/212	03/108	343/87	45/82	50/82	325/87	544/80	42/82	43/82	00/212
SiO_2	41.48	41.29	40.53	41.28	42.03	40.59	40.69	40.19	40.98	41.44	53.87	55.09	54.40	55.81	54.86	55.21	54.47	55.00
TiO_2	<0.10	0.11	<0.10	<0.10	<0.10	<0.10	–	–	<0.10	<0.10	0.26	0.13	<0.11	<0.11	<0.11	<0.05	<0.05	<0.05
Al_2O_3	19.26	18.78	21.18	19.54	21.46	19.05	19.54	19.66	19.06	18.32	4.02	2.96	1.81	2.32	1.11	1.72	1.60	1.01
Cr_2O_3	6.37	6.35	3.14	5.25	3.18	5.98	4.78	5.06	5.16	6.85	4.41	1.46	1.44	1.41	1.18	1.46	1.25	1.07
FeO	7.88	7.80	9.72	8.12	7.75	7.93	7.84	8.06	7.46	8.03	3.15	1.64	1.39	1.86	1.41	1.28	1.35	1.70
MnO	0.47	0.55	0.56	0.46	0.36	0.40	0.43	0.44	0.40	0.34	<0.10	<0.11	<0.10	0.10	<0.10	–	–	<0.06
MgO	20.23	19.37	19.56	19.08	20.02	19.14	18.53	18.16	19.24	18.65	13.10	15.95	16.90	17.88	17.59	16.73	16.58	17.88
CaO	4.65	5.43	5.20	6.38	5.24	6.44	6.06	6.39	5.85	6.35	16.85	21.11	22.00	19.39	22.76	21.76	21.36	22.16
Na_2O	0.07	<0.05	<0.05	<0.05	<0.05	<0.05	n.a.	n.a.	n.a.	<0.05	3.93	1.81	1.46	1.71	1.04	0.55	0.80	0.90
K_2O	<0.07	<0.07	<0.07	<0.07	<0.07	<0.07	n.a.	n.a.	n.a.	<0.07	<0.07	<0.07	<0.07	<0.07	<0.07	n.a.	n.a.	n.a.
NiO	0.12	<0.08	<0.08	<0.08	<0.08	0.09	n.a.	n.a.	n.a.	<0.08	<0.08	<0.07	<0.08	<0.08	<0.08	n.a.	n.a.	<0.06
Total	100.53	99.68	99.89	100.11	100.04	99.61	97.87	97.96	98.15	99.98	99.58	100.15	99.39	100.49	99.95	98.71	97.41	99.72
Rb	8.33	8.23	n.a.	7.97	7.26	7.44	n.a.	n.a.	n.a.	7.61	4.76	2.48	2.44	2.97	5.20	n.a.	n.a.	1.99
Sr	0.65	1.4	n.a.	0.51	0.069	0.15	n.a.	n.a.	0.065	0.28	430.1	394.3	144.6	11.6	0.52	n.a.	n.a.	4.81
Ba	0.36	0.304	n.a.	0.23	0.015	0.076	n.a.	n.a.	0.004	0.06	2.34	2.00	21.18	2.42	0.045	n.a.	n.a.	45.00
Nb	0.49	0.61	0.302	0.72	0.21	0.37	0.30	0.35	0.31	0.48	4.25	0.50	0.97	0.64	0.013	0.35	0.36	0.22
Zr	23.59	39.45	9.09	1.94	0.20	0.16	0.18	0.24	0.12	0.18	119.29	3.32	0.72	0.37	0.043	0.26	0.30	0.47
Hf	0.51	0.67	0.159	0.065	0.085	–	0.012	0.006	0.06	–	2.84	0.10	0.021	0.017	0.006	0.002	0.002	0.022
Ti	636.2	596.8	409.3	154.3	81.1	13.6	19.3	30.1	15.0	4.1	763.1	494.5	84.6	94.2	3.8	27.9	32.2	16.9
La	0.067	0.209	0.011	0.084	0.008	0.024	0.004	0.002	0.017	0.117	18.90	13.94	6.56	0.65	0.005	0.001	0.046	1.10
Ce	0.91	1.68	0.15	1.02	0.065	0.012	0.009	0.008	0.054	0.046	70.67	40.33	17.83	1.37	0.009	0.004	0.127	1.40
Nd	4.80	4.34	1.51	2.07	0.058	0.004	0.003	0.005	0.070	–	51.65	20.39	5.66	0.49	0.005	0.002	0.043	0.125
Sm	1.59	1.62	0.96	0.50	0.019	–	0.003	0.006	0.003	–	9.03	2.16	0.34	0.016	–	0.002	0.012	–
Eu	0.39	0.42	0.33	0.12	0.004	0.010	–	0.003	0.001	–	2.12	0.39	0.038	0.007	0.001	–	0.001	0.019
Gd	0.91	1.2	n.a.	0.16	0.012	0.006	n.a.	n.a.	–	0.012	4.61	–	0.050	0.049	0.002	n.a.	n.a.	n.a.
Dy	0.72	0.76	0.50	0.20	0.27	0.008	0.04	0.027	0.007	0.003	1.97	0.19	0.040	0.016	0.006	0.002	0.003	0.002
Y	4.47	2.881	2.51	1.15	3.95	0.17	0.70	0.55	0.22	0.066	3.69	0.35	0.081	0.145	0.009	0.031	0.019	0.015
Er	0.68	0.353	0.36	0.24	0.76	0.02	0.14	0.06	0.04	0.008	0.47	0.07	0.003	0.007	–	0.007	0.001	0.003
Yb	1.14	0.613	0.49	0.52	1.84	0.36	0.37	0.24	0.19	0.174	0.06	0.14	0.030	0.022	–	0.017	0.006	0.022

Note: (n.a.) Not analyzed; (–) below detection limit. Samples 00/212 and 03/108 are from the collection of S.I. Kostrovitskii.

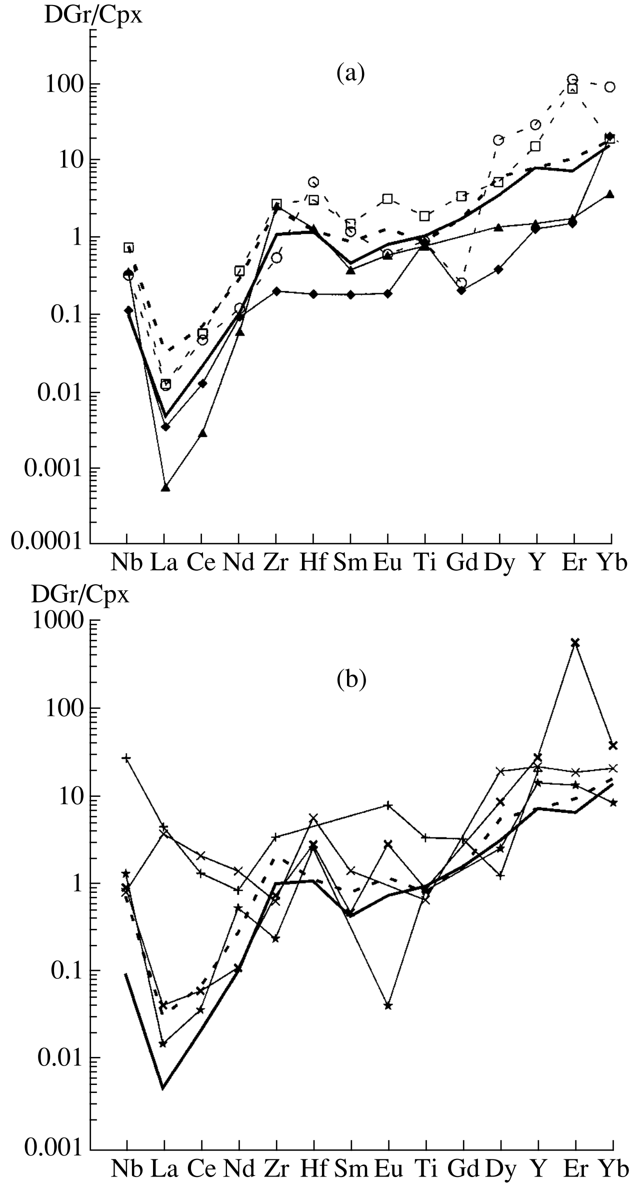

Fig. 2. (a) Coefficients of partition of rare elements (Nb, Zr, Hf, Ti, Y, and REE) between garnet and clinopyroxene (DGr/Cpx) in rocks of (a) groups 1 and 2 and (b) group 3. DGr/Cpx values were calculated as ratios of trace element contents in garnet and clinopyroxene determined in the studied samples. Thick lines are theoretical DGr/Cpx values calculated as ratios of garnet/melt and clinopyroxene/melt partition coefficients based on published data: solid line, after [12] (after [13] for Gd); dashed line, after [13] for Nb, Zr, Hf, Ti, Gd, and Yb; after [1] for La, Ce, Nd, Sm, Eu, Dy, and Er (DGr/L is at 1000°C); and after [12] for Y.

The concentrations of rare elements in garnet and clinopyroxene and their chondrite-normalized patterns do not correlate with the amounts of these minerals in rocks and with the orthopyroxene contents, but reveal a correlation with the contents of orange, brown, and yellow olivine varieties. For example, garnet harzburgites from samples 545/80 (group 1) and 03/108 (group 3) are similar in the modal mineral composition but significantly different in concentration and distribution of rare elements in accordance with the olivine coloration. As has been shown previously [8], orange, brownish, and yellow olivines bear a substantial admixture of ferric ion and remain in the rocks as relict minerals during the percolation of reduced fluids through solid rocks at the early stage of kimberlite formation. The appreciable depletion of pale green and colorless olivines in Fe^{3+} in reference samples [8] testifies to the reduced character of the affecting fluids. The formation of native graphite in mantle metasomatites of reaction type is likely related to precisely such fluids [14]. The reduced character of fluids may be explained by the development of an advanced hydrogen front in asthenospheric melts beneath the lithospheric mantle during the kimberlite-forming cycle [7]. These fluids vigorously extracted incompatible rare elements from rocks and minerals. Probably, they were also responsible for reaction metasomatism at oxidizing geochemical barriers.

The next logical conclusion is no less important. The primary substance of the lithospheric mantle of the Siberian Craton was composed of rocks and minerals enriched in incompatible rare elements rather than depleted in these elements. This suggestion provides new insight into the primary nature of the lithospheric mantle beneath ancient cratons. If the ancient lithospheric mantle was initially enriched in incompatible rare elements, it cannot be regarded as a restite left after the generation of basaltic or komatiitic melts, as is commonly accepted now [5, 6, 11, and others]. It is also thought that the restitic mantle was enriched in incompatible rare elements as a result of introduction of subduction-related silicic melts [15]. In the example considered above, this hypothesis comes into conflict with the absence of a correlation between the rare element contents in garnet and clinopyroxene, on the one hand, and the amount of these minerals and orthopyroxene in rocks, on the other hand. Garnet and clinopyroxene from lherzolite sample 00/212 (group 3) are depleted in rare elements in full agreement with the pale green and colorless character of olivines, though the xenolith is enriched in orthopyroxene and contains a few relict deformed megacrystals of this mineral. If the megacrystals were old porphyroblasts related to the metasomatic impact of a subduction-related silicic melt, the minerals would be enriched in rare elements.

The Nb, (Zr + Hf), and Ti minimums in lines of clinopyroxene and (Zr + Hf) and Ti minimums in lines of garnet from the most enriched granular peridotites are complementary to peaks of these elements in garnet megacrystals in the deformed peridotite and equilibrium melts that existed beneath the lithospheric plate during the kimberlite tectonomagmatic cycle [3]. Therefore, we can suggest that the high-temperature orthopyroxene–olivine cumulate was a protolith of the lithospheric mantle. The parent melt was depleted in HFSE and highly enriched in LREE and LILE owing to the removal of high-pressure majorite and Mg-perovskite. Precisely majorite and Mg-perovskite accumulate HFSE and are sharply depleted in LREE. The cumulative orthopyroxene of the mixed composition was depleted in HFSE. After the subsequent exsolution of garnet and clinopyroxene, these minerals redistributed trace elements according to the DGr/Cpx value (Fig. 2a). The lower position of DGr/Cpx lines for samples 343/87 and 45/82 relative to the theoretical curves might be caused by an exsolution of garnet and clinopyroxene in equilibrium with carbonate liquid.

CONCLUSIONS

The lithospheric mantle of the Siberian Craton was washed out by reduced fluids delivered from asthenospheric magma sources at the early stage of kimberlite formation in the Middle Paleozoic. The ascending fluids intensely extracted incompatible rare elements from rocks and minerals. Subsequently, these elements were precipitated in metasomatites of reaction type at the oxidizing barriers. Metasomatic diamonds and graphite might be products of such a reductive process.

The protolith of the lithospheric mantle was represented by the light olivine–orthopyroxene cumulates crystallized in the ancient magma ocean. They were complementary to the high-pressure majorite–Mg-perovskite buried in the transitional zone of the upper mantle and enriched in HFSE. As a result, the lithospheric protolith was enriched in LREE and LILE and depleted in HFSE.

ACKNOWLEDGMENTS

I thank S.I. Kostrovitskii for the samples kindly placed at my disposal.

This work was supported by the Russian Foundation for Basic Research, project no. 06-05-64756.

REFERENCES

1. S. R. Burgess and B. Harte, J. Petrol. **45**, 609 (2004).
2. A. I. Kiselev, K. N. Egorov, and M. N. Maslovskaya, Otechest. Geol., No. 4, 40 (2002).
3. K. N. Egorov, L. V. Solov'eva, and S. G. Simakin, Dokl. Earth Sci. **397**, 698 (2004) [Dokl. Akad. Nauk **397**, 88 (2004)].
4. D. Smith and F. R. Boyd, in *Mantle Xenoliths* (Wiley, Chichester, 1987), pp. 531–561.
5. W. L. Griffin, S. R. Shee, C. G. Ryan, et al., Contrib. Mineral Petrol. **134**, 232 (1999).
6. N. C. Simon, G. L. Irvine, G. R. Davies, et al., Lithos **71**, 289 (2003).
7. L. V. Solov'eva, K. N. Egorov, M. E. Markova, et al., Geol. Geofiz. **38** (1), 172 (1997).
8. L. N. Solovieva, V. G. Barankevich, O. A. Bayukov, and O. M. Glazunov, in *Proceedings of VII Int. Kimberlite Conference* (Cape Town, 1998), pp. 841–843.
9. L. V. Solov'eva, M. A. Gornova, K. N. Egorov, and E. V. Smirnova, Dokl. Earth Sci. **395A**, 456 (2004) [Dokl. Akad. Nauk **395**, 812 (2004)].
10. S.-S. Sun and W. F. McDonough, Geol. Spec. Publ. **42**, 313 (1989).
11. N. Shimizu, N. P. Pokhilenko, F. R. Boyd, and D. G. Pearson, Geol. Geofiz. **38** (1), 194 (1997).
12. K. T. M. Johnson, Contrib. Mineral. Petrol. **133**, 60 (1998).
13. Q. Xie, T. C. McCuaig, and R. Kerrich, Chem. Geol. **126**, 29 (1995).
14. L. V. Solov'eva, S. I. Kostrovitskii, A. V. Ukhanov, et al., Dokl. Earth Sci. **385**, 589 (2002) [Dokl. Akad. Nauk **385**, 231 (2002)].
15. P. B. Kelemen, S. R. Hart, and S. Bernstein, Earth Planet. Sci . Lett. **164**, 387 (1998).